# Crystalline Orientation in Syndiotactic Polystyrene Cast Films

**Paola Rizzo,*,† Marina Lamberti,† Alexandra R. Albunia,† Odda Ruiz de Ballesteros,‡ and Gaetano Guerra†**

*Dipartimento di Chimica, Università degli Studi di Salerno, Via S. Allende, 84081 Baronissi (Salerno), Italy; and Dipartimento di Chimica, Università degli Studi di Napoli "Federico II", Complesso di Monte Sant'Angelo Via Cinthia, 80126 Napoli, Italy*

*Received October 24, 2001; Revised Manuscript Received February 13, 2002*

ABSTRACT: The kind and degree of crystalline phase orientation for clathrate s-PS films, obtained by solution-casting procedures, and for semicrystalline films, obtained by suitable treatments on these cast films, are analyzed. Clathrate as well as nanoporous form films can present high degrees of uniplanar orientation, corresponding to the tendency of the *ac* crystallographic planes, to be parallel to the film plane. The driving force for this kind of orientation is the tendency of rows of parallel **s**(2/1)2 helices with minimum interchain and maximum interplanar distances to be parallel to the film plane. A high degree of uniplanar orientation is also maintained after annealing procedures leading to $\gamma$ form, that is the other crystalline form which presents the same helical conformation. A tentative indexing of the $\gamma$ form reflections, based on an orthorhombic unit cell, again indicates the presence of parallelism of *ac* planes with respect to the film surface. A substantial planar orientation, corresponding to the placement of the chain axes parallel to the film plane can also be maintained after annealing procedures at higher temperatures (220−230 °C) leading to $\alpha$ and $\beta$ crystalline forms, where trans-planar rather than helical chains are included.

## Introduction.

Syndiotactic polystyrene (s-PS) has a number of properties, which are different from those of conventional styrenics, and are superior for practical applications: it has a very high melting point (close to 270 °C), high crystallization rate, and high chemical stability as well as excellent processability in most thermoplastic fabrication technologies.

s-PS presents a very complex polymorphic behavior.[1,2] Four different crystalline forms have been described. By melt crystallization procedures both high melting $\alpha$[3−5] and $\beta$[6−8] forms, which are characterized by chains in the trans-planar conformation, can be obtained. By solution crystallization procedures, besides the $\beta$ form, the thermally unstable $\gamma$ and $\delta$ forms as well as clathrate forms, all including chains in the **s**(2/1)2 helical conformation, can be obtained.

Both $\alpha$ and $\beta$ forms can exist in different modifications having different degrees of structural order, so that two limit-disordered modifications ($\alpha'$ and $\beta'$) and two limit-ordered modifications ($\alpha''$ and $\beta''$) have been described[1,3−7]. In particular the disorder present in the $\alpha'$ modifications would correspond to the statistical occurrence of two specific orientations of triplets of chains,[7] whereas the disorder present in the $\beta'$ modifications would refer to the stacking of ordered macromolecular bilayers.[6] Besides the four crystalline forms, two mesomorphic forms of s-PS, containing chains in the trans-planar[9−11] and **s**(2/1)2 helical conformations[12] have been also described.

In all the described s-PS clathrate phases, **s**(2/1)2 helices (the host) form a crystal lattice containing spaces in which molecules of a second chemical species (the guest) are located. Semicrystalline samples including clathrate phases can be obtained, by solution crystallization or by sorption of suitable compounds (e.g., methylene chloride, toluene, chloroform, etc.) in amorphous s-PS samples as well as in semicrystalline s-PS samples in the $\alpha$, $\gamma$, or $\delta$ form. For these clathrate structures, the intensities and the precise locations of the reflections in X-ray diffraction patterns only slightly change with the kind and the amount of the included guest molecules.[1,13] The crystal structures of clathrate phases including, as guest molecules, toluene,[14] iodine[15] or 1,2-dichloroethane,[16] which have been determined with good accuracy, are in fact all similar to each other.

The $\gamma$ form, whose structure is still unknown, can be obtained by solution crystallization procedures involving solvents which are not able to form clathrate phases (as bromooctane, nonane, decane, etc.) or by annealing of $\delta$ or clathrate forms in the temperature range 110−170 °C.[1,12]

The $\delta$ form, which can be obtained by suitable guest extraction procedures on samples in all clathrate forms,[12,17,18] presents a structure similar to those of the s-PS clathrates, but in place of the guest molecules, it includes two identical cavities per unit cell,[19] whose shape and volume have been thoroughly characterized.[20] s-PS samples in the nanoporous $\delta$ form rapidly absorb suitable volatile organic compounds and transform into the corresponding clathrate forms.

Sorption studies have suggested that nanoporous $\delta$ form samples are promising for applications in chemical separations as well as in water and air purification.[21,22] In particular, thin polymeric films have been suggested as sensing elements of molecular sensors.[23]

It is well-known that molecular diffusion through polymeric films is markedly dependent on the presence of macromolecular orientation.[24] Diffusion is expected to be particularly dependent on the orientation of the crystalline phase, for these nanoporous materials which absorb molecules, mainly as guests in that phase.[22,25,26]

† Università degli Studi di Salerno.
‡ Università degli Studi di Napoli "Federico II".

10.1021/ma011853u CCC: $22.00 
Published on Web 06/12/2002

Of course, as generally occurs for semicrystalline polymers, especially for low thickness applications, the crystalline orientation, together with the amorphous orientation, is also relevant to physical properties of s-PS samples in all crystalline forms.

In this paper, the kind and the degree of crystalline phase orientation for clathrate s-PS films, obtained by solution-casting procedures, and for semicrystalline films, obtained by suitable treatments on these cast films, are analyzed.

As for the terminology relative to the crystalline phase orientation we will use the definitions by Heffelfinger and Burton[27] for which an orientation is named uniplanar when a crystal plane is parallel to a reference plane, whereas is planar when a crystal axis is lying in a reference plane.

## Experimental Section

The s-PS used in this study was manufactured by Dow Chemical Co. under the trademark Questra 101. The $^{13}C$ nuclear magnetic resonance characterization showed that the content of syndiotactic triads was over 98%. The weight-average molar mass obtained by gel permeation chromatography (GPC) in trichlorobenzene at 135 °C was found to be $M_w = 3.2 \times 10^5$ with the polydispersity index $M_w/M_n = 3.9$.

Chloroform clathrate films, 25−40 $\mu$m thick, were obtained by casting procedure from a 1% w/w solution in chloroform at room temperature.

$\delta$ semicrystalline films were obtained by exposing chloroform clathrate film to vapors of $CS_2$ and by subsequent drying at 50 °C under vacuum. 1,2-Dichloroethane (DCE) clathrate films ($\delta_{DCE}$) were obtained by exposing chloroform clathrate films to 1,2-dichloroethane vapor at room temperature.

$\gamma$ and $\alpha$ semicrystalline films were obtained from chloroform clathrate films by increasing the temperature ($\approx$ 2 °C/min) from room temperature up to 160 and 220 °C, respectively, and then maintaining the samples at that temperature for 30 min. $\beta'$ semicrystalline films were obtained by inserting chloroform clathrate films in an oven hold at 230 °C and then by annealing the samples at that temperature for 30 min.

Unoriented samples of Figure 1 were obtained by following procedures analogous to those described in detail in refs 1 and 20.

Fiber samples in the $\alpha$ form, used as reference in Table 5, were obtained by stretching at 150 °C extruded samples. Fiber samples in $\delta_{DCE}$, $\delta$, $\gamma$, and $\beta$ forms, used as reference in Tables 1−4, were obtained by exposure to DCE vapor of $\alpha$-form fibers and subsequent suitable treatments.

Wide-angle X-ray diffraction patterns with nickel-filtered Cu K$\alpha$ radiation were obtained, in reflection, with an automatic Philips diffractometer as well as, in transmission, by using a cylindrical camera (radius = 57.3 mm). In the latter case the patterns were recorded on a BAS-MS Imaging Plate (FUJIFILM) and processed with a digital imaging reader (FUJIBAS 1800). In particular, to recognize the kind of crystalline orientation present in the samples, photographic X-ray diffraction patterns were taken with X-ray beam both perpendicular and parallel to the film surface.

The degree of uniplanar orientation for $\delta_{DCE}$, $\delta$, and $\gamma$ forms (parallelism of crystallographic planes (0$k$0) to the film plane) and of planar orientation for $\beta$ and $\alpha$ forms (parallelism of the chain axis to the film plane)[27] have been formalized on a quantitative numerical basis using Hermans' orientation function, $f_x$[28,29]

$$f_x = (3\overline{\cos^2 x} - 1)/2 \qquad (1)$$

by assuming $\overline{\cos^2 x}$ as the squared average cosine value of the angle, $x$, between the normal to the film surface and the normal to the (0$k$0) crystallographic plane for the uniplanar orientation, and between the film surface and the chain axis $c$ for the planar orientation.

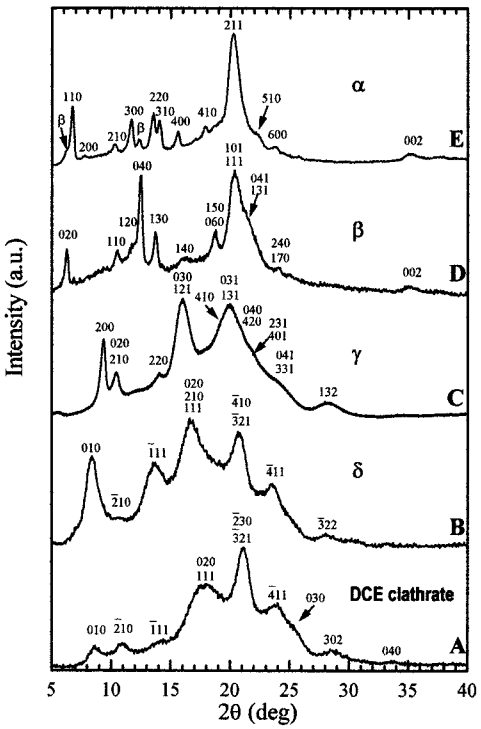


**Figure 1.** Typical X-ray diffraction patterns obtained with nickel-filtered Cu K$\alpha$ radiation with an automatic Philips diffractometer of unoriented s-PS samples including $\delta_{DCE}$ (A), $\delta$ (B), $\gamma$ (C), $\beta$ (D), and $\alpha$ (E) forms. In particular, for $\alpha$ and $\beta$ forms, X-ray diffraction patterns which include also peaks of the limit-ordered modifications $\beta''$ and $\alpha''$ have been reported. The Miller indexes of the most intense reflections are indicated near to the peaks. As for the $\gamma$ form, tentative Miller indexes have been indicated (see text).

Since, in our cases, a $\theta_{hkl}$ incidence of X-ray beam is used, the quantity $\overline{\cos^2 x}$ can be easily experimentally evaluated. In particular, as for the uniplanar orientation of $\delta_{DCE}$, $\delta$, and $\gamma$ forms

$$\overline{\cos^2 x} = \overline{\cos^2 \chi_{0k0}} = \frac{\int_0^{\pi/2} I(\chi_{0k0}) \cos^2 \chi_{0k0} \sin \chi_{0k0} \, d\chi_{0k0}}{\int_0^{\pi/2} I(\chi_{0k0}) \sin \chi_{0k0} \, d\chi_{0k0}} \qquad (2)$$

where $I(\chi_{0k0})$ is the intensity distribution of a (0$k$0) diffraction on the Debye ring as collected by sending the X-ray beam parallel to the film surface, $\chi_{0k0}$ is the azimuthal angle measured from the equator, that is the line defined by the (0$k$0) reflections.

As for the planar orientation of $\alpha$ and $\beta$ forms

$$\overline{\cos^2 x} = \overline{\cos^2 \chi_{002}} = \frac{\int_0^{\pi/2} I(\chi_{002}) \cos^2 \chi_{002} \sin \chi_{002} \, d\chi_{002}}{\int_0^{\pi/2} I(\chi_{002}) \sin \chi_{002} d\chi_{002}} \qquad (3)$$

where $I(\chi_{002})$ is the intensity distribution of the (002) diffractions on the Debye rings as collected by sending the X-ray beam parallel to the film surface, $\chi_{002}$ is the azimuthal angle measured from the meridian, in this case the equator is the line defined by the ($hk$0) reflections.

The diffracted intensities $I(\chi_{hkl})$ of equation[2,3] were obtained, in transmission, by using an AFC7S Rigaku automatic diffractometer (with a monochromatic Cu K$\alpha$ radiation) and maintaining an equatorial geometry. Because the collection

**Table 1. Comparison between the Relative Intensities of the Reflections of the DCE Clathrate Form ($\delta_{DCE}$) Observed in X-ray Diffraction Patterns for Cast Films (Collected with Beams Perpendicular (⊥) and Parallel (∥) to the Film Plane) as Well as for Fibers[a]**

| | fiber | | film | | | |
|---|---|---|---|---|---|---|
| *hkl* | $2\theta_{obs}$ | $I_{obs}$ | $I_{obs}(\perp)$ | $I_{obs}(\parallel)$ | $\chi_{obs}$, deg | $\chi_{calcd}$, deg |
| 010 | 8.50 | s | | vs | 0 | 0 |
| $\bar{2}10$ | 10.75 | s | s | mw | 75 ± 10 | 77 |
| 020 | 17.0 | w | | mw | 0 | 0 |
| 210 | | | | mw | 36 ± 10 | 36 |
| $\bar{4}10$ | 21.0 | m | s | | | 80 |
| $\bar{4}20$ | | | | | | 77 |
| $\bar{2}30$ | | | | w | 38 ± 10 | 28 |
| 220 | 25.5 | mw | | | 24 | |
| 030 | | | | w | 0 | 0 |
| $\bar{6}10$ | 33.6 | w | | | | 73 |
| 230 | | | | | | 18 |
| 040 | | | | vvw | 0 | 0 |
| $\bar{1}11$ | 13.7 | w | vvw | vw | 65 ± 10 | 67 |
| 111 | 17.5 | s | vvw | | | 48 |
| $\bar{1}21$ | | | | ms | 43 ± 15 | 42 |
| $\bar{2}21$ | | | | | | 55 |
| $\bar{3}21$ | 21.3 | vs | s | s | 60 ± 10 | 68 |
| 301 | | | | | | 65 |
| 211 | | | | w | 38 ± 10 | 47 |
| 121 | 24.3 | s | ms | | 33 | |
| $\bar{4}11$ | | | | m | 75 ± 10 | 81 |
| $\bar{4}21$ | | | | | | 78 |
| $\bar{3}31$ | 26.5 | m | | | | 50 |
| $\bar{1}31$ | | | | vvw | 38 ± 10 | 30 |
| 311 | | | | | | 48 |
| $\bar{1}12$ | 25.5 | s | w | | | 77 |
| 012 | | | | vvw | 75 ± 10 | 70 |
| $\bar{2}12$ | | | | | | 85 |
| 022 | 29.3 | s | vw | | | 54 |
| $\bar{3}22$ | | | | vvw | 75 ± 10 | 74 |
| 212 | | | | | | 60 |
| 302 | | | | | | 72 |

[a] As for the patterns collected with beam parallel to the film plane, the observed azimuthal angles ($\chi_{obs}$) are compared to those calculated ($\chi_{calcd}$) in the assumption of complete parallelism of the (010) planes with respect to the film plane.

was performed at constant $2\theta$ values and in the equatorial geometry, the Lorentz and polarization corrections were unnecessary.

In these assumptions, for the uniplanar orientation, $f_x = f_{0k0}$ is equal to 1 if (0$k$0) planes of all crystallites are perfectly parallel to the plane of the film, whereas it is equal to −0.5 if the (0$k$0) planes are perpendicular to it. As for the planar orientation, $f_x = fc$ is equal to 1 if the $c$ axes of all crystallites are perfectly lying on the film plane, while $fc$ is equal to −0.5 if the $c$ axes of all crystallites are perpendicular to the film plane.

The calculated angles ($\chi_{calcd}$) between each crystallographic plane and the $ac$ plane for the monoclinic $\delta$ and $\delta_{DCE}$ forms and for the orthorhombic $\gamma$ form, which are reported in Tables 1−3, have been determined by using eqs 4 and 5, respectively:

$$\chi_{hkl} = \arccos\left( d_{hkl}\left(h\frac{\cos\gamma}{a\sin\gamma} + k\frac{-1}{b\sin\gamma}\right)\right) \quad (4)$$

$$\chi_{hkl} = \arccos\left(d_{hkl}\left(k\frac{-1}{b}\right)\right) \quad (5)$$

## Results and Discussion

Typical X-ray diffraction patterns obtained by an automatic powder diffractometer of unoriented semicrystalline s-PS samples presenting 1,2-dichloroethane clathrate ($\delta_{DCE}$) $\delta$, $\gamma$, $\beta$, and α forms are reported in Figure 1. In particular, for α and $\beta$ forms, to have all possible reflections, X-ray diffraction patterns which include also peaks of the limit-ordered modifications $\beta''$ and α″ have been reported. The Miller indexes of the calculated most intense reflections for the known $\delta_{DCE}$

**Table 2. Comparison between the Relative Intensities of the Reflections of the $\delta$ Form Observed in X-ray Diffraction Patterns for Dessicated Cast Films (Collected with Beams Perpendicular (⊥) and Parallel (∥) to the Film Plane) as Well as for Fibers[a]**

| | fiber | | film | | | |
|---|---|---|---|---|---|---|
| *hkl* | $2\theta_{obs}$ | $I_{obs}$ | $I_{obs}(\perp)$ | $I_{obs}(\parallel)$ | $\chi_{obs}$, deg | $\chi_{calcd}$, deg |
| 010 | 8.37 | vs | | vs | 0 | 0 |
| 210 | 10.6 | vw | vw | vw | 75 ± 10 | 73 |
| $\bar{2}00$ | 11.5 | vw | | | | 63 |
| $\bar{2}20$ | 15.0 | w | | vw | 45 ± 10 | 41 |
| 020 | 17.0 | w | | mw | 0 | 0 |
| $\bar{2}10$ | | w | *b* | m | 40 ± 10 | 37 |
| $\bar{4}10$ | 20.75 | | | m | 75 ± 10 | 84 |
| $\bar{4}20$ | | | | | | 73 |
| 101 | 13.35 | vs | ms | m | 70 ± 10 | 78 |
| $\bar{1}11$ | | | | | | 65 |
| 111 | 16.8 | ms | | ms | 40 ± 10 | 49 |
| 211 | 20.7 | s | ms | ms | | 49 |
| $\bar{3}01$ | | | | | 65 ± 10 | 68 |
| $\bar{3}21$ | | | | | | 65 |
| $\bar{4}11$ | 23.5 | s | ms | m | 80 ± 10 | 85 |
| $\bar{4}21$ | | | | | | |
| $\bar{1}02$ | 24.8 | m | | vvw | 70 ± 10 | 75 |
| $\bar{1}12$ | | | | | | 84 |
| 012 | | | | | | 76 |
| $\bar{2}12$ | | | | | | 70 |
| 202 | | | | | | 83 |
| 112 | | | | | | 78 |
| 212 | 28.7 | mw | vvw | vvw | 90 ± 15 | 65 |
| $\bar{3}02$ | | | | | | 62 |
| $\bar{3}22$ | | | | | | 74 |

[a] As for the patterns collected with beam parallel to the film plane, the observed azimuthal angles ($\chi_{obs}$) are compared to those calculated ($\chi_{calcd}$) in the assumption of complete parallelism of the (010) planes with respect to the film plane. [b] Reflection hidden by the strong 211, 301 and $\bar{3}21$ reflections.

**Table 3. Comparison between the Relative Intensities of the Reflections of the $\gamma$ Form Observed in X-ray Diffraction Patterns for Annealed Cast Films (Collected with Beams Perpendicular (⊥) and Parallel (∥) to the Film Plane) as Well as for Fibers[a]**

| | fiber | | film | | | |
|---|---|---|---|---|---|---|
| *hkl* | $2\theta_{obs}$ | $I_{obs}$ | $I_{obs}(\perp)$ | $I_{obs}(\parallel)$ | $\chi_{obs}$, deg | $\chi_{calcd}$, deg |
| 200 | 9.25 | s | s | s | 90 | 90 |
| 020 | 10.5 | m | | vs | 0 | 0 |
| 210 | | | | | | 61 |
| 220 | 14.0 | mw | | vw | 45 ± 5 | 42 |
| 030 | 15.75 | mw | | s | 0 | 0 |
| 410 | 19.25 | m | | m | 70 | 74 |
| 040 | 21.25 | mw | | m | 0 | 0 |
| 420 | | | | m | 60 ± 10 | 61 |
| 240 | 23 | w | | w | 15 ± 10 | 24 |
| 121 | 16.25 | vs | vw | s | 50 ± 10 | 50 |
| 031 | 19.94 | s | ms | m | 32 ± 10 | 36 |
| 131 | | | | m | 38 ± 10 | 38 |
| 231 | 21.66 | mw | m | | | 43 |
| 401 | | | | w | 85 ± 5 | 90 |
| 041 | 23.81 | mw | vvw | | | 29 |
| 331 | | | | | | 49 |
| 202 | 25.02 | m | | | | 90 |
| 022 | | | | vw | 73 ± 10 | 66 |
| 212 | | | | | | 78 |
| 132 | 28.48 | m | m | vw | 70 ± 10 | 56 |

[a] As for the patterns collected with beam parallel to the film plane, the observed azimuthal angles ($\chi_{obs}$) are compared to those calculated ($\chi_{calcd}$) in the assumption of complete parallelism of the (0$k$0) planes with respect to the film plane.

**Table 4. Comparison between the Relative Intensities of the Reflections of the $\beta$ Form Observed in X-ray Diffraction Patterns for Annealed Cast Films (Collected with Beams Perpendicular (⊥) and Parallel (∥) to the Film Plane) as Well as for Fibers**

| | fiber | | film | |
|---|---|---|---|---|
| *hkl* | $2\theta_{obs}$ | $I_{obs}$ | $I_{obs}(\perp)$ | $I_{obs}(\parallel)$ |
| 020 | 6.15 | ms | mw | s |
| 110 | 10.45 | w | | mw |
| 120[b] | 11.80 | m | | vw |
| 040 | 12.35 | s | m | vs |
| 130 | 13.60 | m | mw | ms |
| 140[b] | 15.90 | mw | | vvw |
| 150 | 18.50 | m | w | ms |
| 060 | | | | |
| 200[b] | 20.15 | m | *a* | mw |
| 230[b] | 22.21 | mw | | vvw |
| 170 | 23.90 | w | | mw |
| 080 | 25.15 | vw | | vvw |
| 250 | | | | |
| 111 | 20.60 | vs | vs | s |
| 041 | 21.40 | ms | ms | m |
| 002 | 35.50 | mw | mw | w |
| 132 | 37.50 | mw | mw | w |

[a] Reflection hidden by the very strong 111 reflection. [b] Reflections typical of the limit ordered $\beta''$ modification.

**Table 5. Comparison between the Relative Intensities of the Reflections of the α Form Observed in X-ray Diffraction Patterns for Annealed Cast Films (Collected with Beams Perpendicular (⊥) and Parallel (∥) to the Film Plane) as Well as for Fibers**

| | fiber | | film | |
|---|---|---|---|---|
| *hkl* | $2\theta_{obs}$ | $I_{obs}$ | $I_{obs}(\perp)$ | $I_{obs}(\parallel)$ |
| 110 | 6.70 | s | m | s |
| 200 | 7.82 | vw | | vvw |
| 210 | 10.3 | m | | w |
| 300 | 11.7 | s | m | s |
| 040[b] | 12.35 | | | mw |
| 220 | 13.6 | s | m | s |
| 310 | | | | w |
| 400 | 15.6 | m | w | w |
| 410 | 17.8 | m | | w |
| 330 | 20.5 | m | *a* | mw |
| 420 | | | | |
| 510 | 21.6 | w | | vw |
| 600 | 23.8 | m | | w |
| 430 | | | | |
| 211 | 20.4 | vs | vs | s |
| 002 | 35.8 | m | m | m |
| 102 | | | | |

[a] Reflection hidden by the very strong 211 reflection. [b] Reflections typical of the $\beta$ form.

$\delta$, $\beta$, and α crystalline structures are indicated near to the peaks. As for the $\gamma$ form, on the basis of an orthorhombic unit cell with parameters $a = 19.15$ Å, $b = 17.0$ Å, and $c = 7.7$ Å derived by electron diffraction measurements on single crystals,[30] Miller indexes are also indicated.

X-ray diffraction patterns by automatic powder diffractometer of s-PS films, all obtained by casting followed by exposition to DCE vapors ($\delta_{DCE}$ form) or to $CS_2$ vapors and by subsequent drying at 50 °C under vacuum ($\delta$ form), by annealing at 160 ($\gamma$ form) or at 220 °C (α form), or by abrupt annealing at 230 °C ($\beta$ form), are reported in Figure 2; the Miller indexes are also indicated.

The occurrence of strong molecular orientation is clearly pointed out by the substantial variation of the

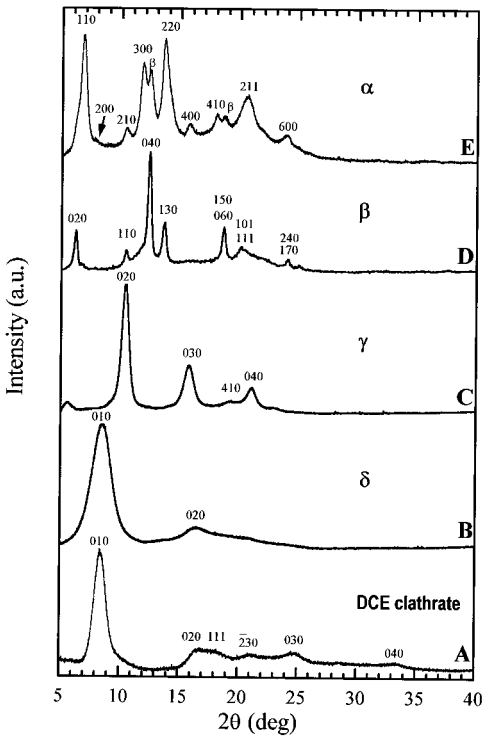


**Figure 2.** X-ray diffraction patterns of s-PS films obtained by casting from chloroform solutions treated under different conditions: (A) exposure to DCE vapors, $\delta_{DCE}$ clathrate form; (B) exposure to $CS_2$ vapors and subsequent drying at 50 °C under vacuum, $\delta$ form; (C) annealing at 160 °C, $\gamma$ form; (D) abrupt annealing at 230 °C, $\beta$ form; (E) slow annealing at 220 °C, α form. The Miller indexes are also indicated.

reflection intensities with respect to the unoriented samples of Figure 1. In particular, for $\delta$ and $\delta_{DCE}$ forms the (010) remains the only intense reflection, while the (020), which is not detectable in unoriented samples, becomes second in intensity. This suggests an orientation of *ac* planes prevailingly parallel to the film plane. X-ray diffraction patterns of oriented clathrate films obtained by casting, analogous to the one shown in Figure 2A, have been already reported in ref 22.

As for the $\gamma$ crystalline form, it is apparent that the only intense reflections remain those with possible Miller indexes (020), (030), and (040). This suggests again an orientation of the *ac* planes mainly parallel to the film plane.

For both α and $\beta$ crystalline forms, by comparison with the patterns of unoriented samples (Figure 1D,E), it is apparent that layer line reflections tend to be reduced with respect to all equatorial reflections. This suggests the tendency of the *c* axes to remain nearly parallel to the film plane.

A better understanding of the crystalline orientation present in these films, can be achieved by X-ray patterns taken with beams perpendicular and parallel to the film plane on a photographic cylindrical camera. The X-ray diffraction patterns collected with beams perpendicular to the film plane show only Debye Sherrer rings, indicating that there is not any axial orientation in the film plane. The corresponding X-ray diffraction profiles obtained by a digital imaging reader are reported in Figure 3, parts A−E.

X-ray patterns collected with beams parallel to the film plane are reported in Figure 4, parts A−E, respectively; different from the patterns obtained with beams perpendicular to the film plane, arcs rather than Debye

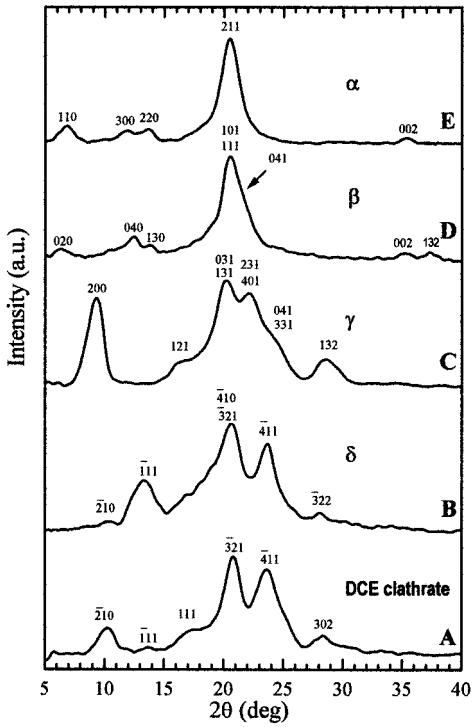


**Figure 3.** X-ray diffraction patterns of the same films of Figure 2 obtained with beams perpendicular to the film plane by using a photographic cylindrical camera, recorded on a imaging plate and processed with a digital imaging reader.

Sherrer rings are apparent. For patterns collected with both perpendicular and parallel beams, the observed reflections and their relative intensities are reported in Tables 1−5, for oriented $\delta_{DCE}$, $\delta$, $\gamma$, $\beta$, and α films, respectively.

As for $\delta$ and $\delta_{DCE}$ forms, X-ray diffraction patterns obtained with beam parallel to the film plane (Figure 4A,B and fifth column of Tables 1 and 2) show a very intense reflection due to the (010) crystallographic planes, which disappears in X-ray diffraction patterns obtained with beam perpendicular to the film plane (Figure 3A,B and fourth column of Tables 1 and 2). This again suggests that the (010) planes (i.e., the *ac* planes) of the crystallites are characterized by an orientation distribution, whose maximum corresponds to parallelism to the film plane.

For relevant reflections of $\delta$ and $\delta_{DCE}$ forms, the azimuthal angles of maximum intensity ($\chi_{obs}$) which are observed for patterns with beam parallel to the film surface and measured from the equator have been compared with those calculated in the assumption of complete parallelism of the (010) planes with respect to the film plane ($\chi_{calcd}$) (Tables 1,2); the good agreement indicates the occurrence of this uniplanar orientation for $\delta$ and $\delta_{DCE}$ forms.

As shown, for example, for the $\delta$ crystal structure in Figure 5, the (010) planes present the highest density of atoms. In fact they correspond to rows of parallel helices with minimum interchain distances (8.7 and 8.56 Å, for $\delta$ and $\delta_{DCE}$ structures, respectively) and maximum interplanar distances ($d_{010} = \lambda/2(\sin\theta_{010}) = 10.56$ and 10.4 Å, for $\delta$ and $\delta_{DCE}$, respectively).

Hence, as expected for an hydrocarbon polymer for which the only interchain interactions are of van der Waals type, the crystalline plane which tends to be parallel to the film surface (primary slip plane) is that

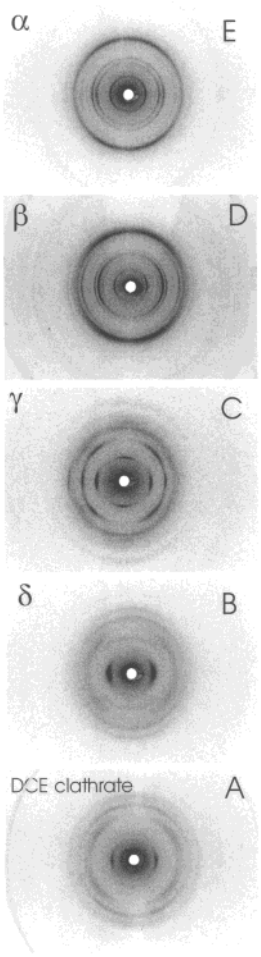


**Figure 4.** X-ray diffraction patterns of the same films of Figure 2 obtained with beams parallel to the film plane by using a photographic cylindrical camera, recorded on a imaging plate.

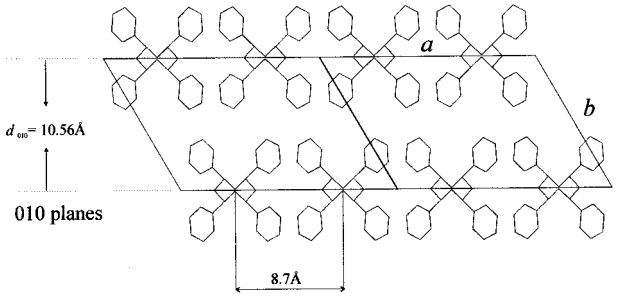


**Figure 5.** Along the chain projections of packing of $\delta$ form of s-PS showing (010) planes which correspond to rows of parallel helices with minimum interchain distances (8.7 Å) and maximum interplanar distances (10.56 Å). These planes tend to be parallel to the film plane for cast films.

one containing the chain axis and having the highest density.

The observed behavior is analogous to that one which has been observed, for instance, for *i*-PP and PET films. In fact, also for these polymers the planes having the highest density of atoms (the (040)[31] and (100) planes,[32] respectively) tend to be parallel to the film surface.

As for the $\gamma$ form a very intense equatorial reflection at $2\theta \approx 10.4°$ possibly due to the (020) crystallographic plane is apparent for the pattern collected with beam parallel to the film plane (Figure 4C and Table 3), whereas the same reflection is practically absent on the

pattern collected with beam perpendicular to the film plane (Figure 3C and Table 3). By comparison of the observed azimuthal angles ($\chi_{obs}$), which are observed for patterns with beam parallel to the film surface and measured from the equator, with those calculated for the case of an ideal uniplanar orientation (see Table 3) it is clearly apparent that the possible (0*k*0) planes tend to be parallel to the film plane also in the $\gamma$ form films.

As for the pattern of the $\gamma$ form obtained with beam parallel to the film plane, it is also worth noting that a meridional reflection, at $2\theta \approx 9.4°$, due to the (200) crystallographic plane, is apparent, strongly supporting the hypothesis, for the $\gamma$ form, of an orthorhombic unit cell.[29]

As for the $\alpha$ and $\beta$ forms, the X-ray diffraction patterns collected with beam parallel to the film plane (Figure 4D,E, Tables 4 and 5) look similar to those of partially oriented fibers; in fact, all the (*hk*0) reflections are equatorial whereas the (*hkl*) are on layer lines.

As for the relative intensities of the reflections observed on the X-ray diffraction pattern collected with beam perpendicular to the film plane (Figure 3D,E), they look altered compared to powder diffraction patterns (Figure 1D,E); in particular, the intensities of the equatorial reflections are reduced with respect to those of the nonequatorial reflections. As for the relative intensities of the reflections observed on the X-ray diffraction pattern collected with beam parallel to the film plane (Tables 4 and 5) a decrease of the nonequatorial reflection with respect to the fiber pattern occurs.

These results, like those of the previous section, indicate that the orientation occurring for the $\alpha$ and $\beta$ forms is essentially a planar orientation with the chain axes, which tend to be parallel to the film plane.

Hence, the phase transitions form helical forms ($\delta$ and $\gamma$) to trans-planar forms ($\alpha$ and $\beta$) is accompanied by the change in texture from uniplanar to planar. In fact, the conformation and packing rearrangements associated with these phase transitions do not allow the maintenance of any substantial orientation of crystal planes, while the direction of the chain axes of the crystallites remains prevailingly unaltered (nearly parallel to the film surface).

Just as an example, this change in texture from uniplanar to planar for a s-PS film, which occurs as a consequence of the transition from the $\delta$ form toward the $\beta$ form, is schematically shown in Figure 6.

It is also worth noting that the planar orientation, which is present in the $\alpha$ and $\beta$ form films, does not alter the relative intensities of the equatorial reflections. As a consequence X-ray diffraction patterns like those shown in Figure 3, parts D and E, and in Tables 4 and 5 can be used to evaluate the degree of structural order in both $\alpha$ and $\beta$ films. In particular, as for the $\beta$ form film, the absence in the pattern of Figure 2D of the (*hkl*) reflections with $h + k = 2n + 1$ ((120) and (140) typical of $\beta''$ modification[1,6] and shown in Figure 1D) and their weakness in the pattern collected with the beam parallel to the film surface (Table 4) clearly indicate the occurrence of a modification close to the limit-disordered one $\beta'$. As for the $\alpha$ form film, the presence in the pattern of Figure 2E of reflections with $-h + k + l \neq 3n$ ((200), (210), (310), (400), and (510) typical of $\alpha''$ modification[1,3] also shown in Figure 1E) indicates that in our film a modification intermediate between the limit-disordered one ($\alpha'$) and the limit-ordered one ($\alpha''$) is present.

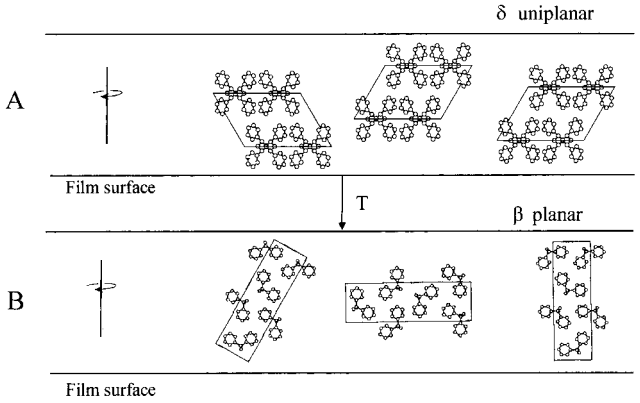


**Figure 6.** Schematic representation of the change of the crystalline phase texture associated with the transition form the helical $\delta$ crystal form toward the trans-planar $\beta$ crystal form. Continues lines correspond to upper and lower surfaces of the films. For the sake of simplicity, only unit cells pointing the chain axes toward the observer are drawn. However as indicated by arrows, a distribution of orientation of unit cells, as determined by their rotation around axes perpendicular to film surface, is present. Key: (A) $\delta$ form unit cells presenting uniplanar orientation ((0*k*0) planes parallel to the film surface); (B) $\beta$ form unit cells presenting planar orientation (*c* axes parallel to the film surface).

**Evaluation of Orientation Factors.** The uniplanar orientation factor for both films in $\delta$ and the $\delta_{DCE}$ forms, evaluated by using Hermans' orientation function, $f_{010}$, (see the Experimental Section), measuring the tendency of the rows of the closest helices to be parallel to the film plane, is 0.76.

For the film in the $\gamma$ form, the uniplanar orientation factor evaluated by using Hermans' orientation function is 0.81, indicating that also after the annealing procedures at ≈160 °C and related structural changes a high degree of orientation is at least maintained. These results suggest that the rows of parallel helices, contained in the (0*k*0) (i.e., *ac*) plane of $\delta$ (shown in Figure 5) and clathrate forms would remain parallel to the film plane, also after transition to the $\gamma$ form although the minimum interchain distance would be increased from 8.7 up to 9.58 Å.

It is worth noting that although the chain conformation changes from $\gamma$ and $\delta$ crystalline forms (**s**(2/1)2 helical conformation) to $\alpha$ and $\beta$ crystalline forms (trans-planar conformation), some crystalline orientation is maintained. In fact, for our films in the $\beta$ and $\alpha$ forms (Figure 4 D,E), the planar orientation factor evaluated by using Hermans' orientation function, $f_{002}$, measuring the tendency of the chain axes to be parallel to the film plane, is 0.51 and 0.70, respectively. It is apparent that while the slow heat treatments leading to the $\alpha$ form reduce only slightly the molecular orientation, the abrupt high-temperature treatments, leading to the $\beta$ form, produce substantial reduction of molecular orientation.

## Conclusions

Clathrate as well as $\delta$ form films obtained by standard casting procedures can present high degree of uniplanar orientation, corresponding to the tendency of the *ac* crystallographic planes, to be parallel to the film plane. The driving force for this kind of orientation is the tendency of rows of parallel **s**(2/1)2 helices with minimum interchain and maximum interplanar distances to be parallel to the film plane.

A high degree of uniplanar orientation is also maintained after annealing procedures leading to $\gamma$ form, that is the other crystalline form which presents the same helical conformation. A tentative indexing of the $\gamma$ form reflections, based on an orthorhombic unit cell, again indicates the presence of parallelism of *ac* planes with respect to the film surface. On this basis, it is reasonable to assume that the rows of helices, parallel to the *ac* planes, which for the $\delta$ (see Figure 5) and clathrate forms are nearly parallel to the film surface, would maintain such parallelism also for the annealed $\gamma$ form films, although the minimum interchain distance would be increased from 8.7 up to 9.58 Å.

This information, as well as the additional reflection data available from samples presenting uniplanar orientation, can contribute to the resolution of the still unknown $\gamma$ form crystalline structure.

A substantial orientation, can also be maintained after annealing procedures at higher temperatures (220−230 °C) leading to $\alpha$ and $\beta$ crystalline forms. In particular, the change in chain conformation form helical (for $\delta$ and $\gamma$ forms) to trans-planar ($\alpha$ and $\beta$ forms) is accompanied by the change in texture from uniplanar to planar corresponding to the placement of the chain axes parallel to the film plane.

The precise knowledge of the crystalline orientation is particularly relevant for $\delta$ form s-PS films for a possible control of the permeability of small molecules through these nanoporous films which is presently investigated by theoretical[33] and experimental studies in our laboratories.

Different kinds of orientations of s-PS crystalline forms, obtained by different preparation procedures, will be described in a paper in preparation.

**Acknowledgment.** Financtial support of the "Ministero dell'Istruzione, del'Università e della Ricerca" (Prin 2000 and Cluster 26) is gratefully acknowledged.

## References and Notes

(1) Guerra, G.; Vitagliano, V. M.; De Rosa, C.; Petraccone, V.; Corradini, P. *Macromolecules* **1990**, *23*, 1539.
(2) Chatani, Y.; Shimane, Y.; Inoue, Y.; Inagaki, T.; Ishioka, T.; Ijitsu, T.; Yukinari, T. *Polymer* **1992**, *33*, 488.
(3) De Rosa, C.; Guerra, G.; Petraccone, V.; Corradini, P. *Polym. J.* **1991**, *23*, 1435.
(4) De Rosa, C. *Macromolecules* **1996**, *29*, 8460.
(5) Cartier, L.; Okihara, T.; Lotz, B. *Macromolecules* **1998**, *31*, 3303.
(6) De Rosa, C.; Rapacciuolo, M.; Guerra, G.; Petraccone, V.; Corradini, P. *Polymer* **1992**, *33*, 1423.
(7) De Rosa, C.; Guerra, G.; Corradini, P. *Rend. Fis. Acc. Lincei* **1991**, *2*, 227.
(8) Chatani, Y.; Shimane, Y.; Ijitsu, T.; Yukinari, T. *Polymer* **1993**, *34*, 1625.
(9) De Candia, F.; Filho, A. R.; Vittoria, V. *Makromol. Chem. Rapid Commun.* **1991**, *12*, 295.
(10) Petraccone, V.; Auriemma, F.; Dal Poggetto, F.; De Rosa, C.; Guerra, G.; Corradini, P. *Makromol. Chem.* **1993**, *194*, 1335.
(11) Auriemma, F.; Petraccone, V.; Dal Poggetto, F.; De Rosa, C.; Guerra, G.; Manfredi, C.; Corradini, P. *Macromolecules* **1993**, *26*, 3772.
(12) Manfredi, C.; De Rosa, C.; Guerra, G.; Rapacciuolo, M.; Auriemma, F.; Corradini, P. *Macromol. Chem. Phys.* **1995**, *196*, 2795.
(13) Immirzi, A.; De Candia, F.; Iannelli, P.; Vittoria, V.; Zambelli, A. *Makromol. Chem. Rapid Commun.* **1988**, *9*, 761.
(14) Chatani, Y.; Shimane, Y.; Inagaki, T.; Ijitsu, T.; Yukinari, T.; Shikuma, H. *Polymer* **1993**, *34*, 1620.
(15) Chatani, Y.; Inagaki, T.; Shimane, Y.; Shikuma, H. *Polymer* **1993**, *34*, 4841.
(16) (a) De Rosa, C.; Rizzo, P.; Ruiz de Ballesteros, O.; Petraccone, V.; Guerra, G.*Polymer*, **1999**, *40*, 2103. (b) De Rosa, C.; Rizzo, P.; Ruiz de Ballesteros, O.; Petraccone, V.; Guerra, G. *Polymer*, **1999**, *40*, 3895.
(17) Guerra, G.; Manfredi, C.; Rapacciuolo, M.; Corradini, P.; Mensitieri, G.; Del Nobile M. A. Ital. Pat., 1994 (C.N.R.).
(18) (a) Guerra, G.; Reverchon, E.; Venditto, V. It. Pat. No. SA98A8. *(*b) Reverchon, E.; Guerra, G.; Venditto, V. *J. Appl. Polym. Sci.* **1999**, *74*, 2077.
(19) De Rosa, C.; Guerra, G.; Petraccone, V.; Pirozzi, B. *Macromolecules* **1997**, *30*, 4147.
(20) Milano, G.; Venditto, V.; Guerra, G.; Cavallo, L.; Ciambelli, P.; Sannino, D. *Chem. Mater.* **2001**, *13*, 1506.
(21) Manfredi, C.; Del Nobile, M. A.; Mensitieri, G.; Guerra, G.; Rapacciuolo, M. *J. Polym. Sci., Polym. Phys. Ed.* **1997**, *35*, 133.
(22) Guerra, G.; Milano, G.; Venditto, V.; Musto, P.; De Rosa, C.; Cavallo, L.; *Chem. Mater.* **2000**, *12*, 363.
(23) Guerra, G.; Venditto, V.; Mensitieri, G. It. Pat. No. SA00A23.
(24) Gohil, R. M. *J. Appl. Polym. Sci.* **1993**, *48*, 1649.
(25) Guerra, G.; Manfredi, C.; Musto, P.; Tavone, S. *Macromolecules* **1998**, *31*, 1329.
(26) (a) Musto, P.; Manzari, M.; Guerra, G. *Macromolecules* **1999**, *32*, 2770. (b) Musto, P.; Manzari, M.; Guerra, G. *Macromolecules* **2000**, *33*, 143.
(27) (a) Alexander, L. E. In *X-ray diffraction methods in Polymer science*; Robert E. Krieger: Huntington, NY, 1979; Chapter 4, pp 210−211. (b) Heffelfinger, C. J.; Burton, R. L. *J. Polym. Sci.* **1960**, *47*, 289.
(28) Samuels, R. J. *Structured Polymer Properties*; John Wiley & Sons: New York, 1971; Chapter 2, pp 28−37.
(29) Kakudo, M.; Kasai, N. *X-ray Diffraction by Polymers*; Elsevier: Amsterdam, 1972; Chapter 10, pp 252−259.
(30) Ruiz, O. Unpublished data.
(31) Uejo, H.; Hoshino, S. *J. Appl. Polym. Sci.* **1970**, *14*, 317.
(32) Werner, E. In *Encyclopedia of Polymer Science and Engineering*, 2nd ed.; Janocha, S., Hopper, M. J., Mackenzie, K. J., Eds.; Wiley-Interscience: New York, 1987; Vol. 12, p 193.
(33) Milano, G.; Guerra, G.; Muller Plathe, F. *Chem. Mater.*, in press.

MA011853U